J. Appl. Environ. Biol. Sci., **1(10)382-396, 2011**
© 2011, TextRoad Publication
ISSN: 2090-4215
Journal of Applied Environmental and Biological Sciences
www.textroad.com

Seismicity and Fault Segmentation of Bafq-Baghin Fault System (Central Iran)

Mehran Arian[1*]; Mohsen Pourkermani[2]; Ali Sistanipour[3]; Hamideh Noroozpour[4]

[1,3]Department of Geology, Science and Research Branch, Islamic Azad University, Tehran, Iran
[2]Department of Geology, Islamic Azad University, North Tehran Branch, Iran
[4]Young Researchers Club, Science and Research Branch, Islamic Azad University, Tehran, Iran

ABSTRACT

Bafq- Baghin Mountain extends from northwest to southeast and is situated in Central Iran's southern border. In this region, we can find Quaternary deposits in the form of unfolded layer. The presence of folded rocks of Pliocene shows active stresses in the late Neogene period which is along with other stresses in the late Cenozoic period seems to have had the strongest effect in the present morphology of the region. The main fault of the region is Bafq- Baghin Fault system which holds right-lateral strike slip with a pressure component. Contemporary activities of this fault signify the continuity of stresses up to now.

Ancient deposits, older than Quaternary in this region during different periods, have been folded repeatedly through stronger or weaker intensity. These structures are the result of important Alpine tectonic movements, especially, tectonic movements of the late Cenozoic period. The axis of most of the folds in the region is in northwest-southeast direction lying in the form of a belt of folds among sunken basins. Bafq- Baghin fault seems to be the most important factor of deformation in this region.

In addition, specific morphotectonic features such as linear valleys, diverted drainages, fault scarps, badly crushed zones and springs are results of active tectonics. Field observations and digital processing of satellite data prove the conformity between the faults which are studied in the area and the expected fractures in shear zone. These fractures include conjugated faults of Riedel and Anti-Riedel(R, R'), normal faults(T), faults parallel with the major fault(Y) and faults approximately parallel with the main fault(P).This conformity and existence of right handed En echelon folds indicate the dominance of the convergent strike slip in the region.

60 fault segments have been recognized on Bafq-Baghin fault system. There are several recent epicenters that situated around of a new transverse lineament with NE-SW trending that introduced in this paper as Rafsanjan-Zarand fault system.

Keywords: Central Iran, Strike slip, Seismicity, fault segmentation, Bafq-Baghin fault system.

1-INTRODUCTION

Our aim in this paper is to segmentation and investigates the seismicity of Bafq-Baghin fault system. The studied area is located in southern border of Central Iran and the main fault in the region is Bafq-Baghin Right lateral strike slip Fault, the mechanism of which is in accordance with the main faults around and inside Central Iran. This fault is located in the southwest and is parallel with Kouh banan active and seismic fault. Probably, these faults are two ancient Central Iran's Faults and have different activities in their geological history.

In this paper the digital processing of satellite data is used for a better identification of the fractures in the region and then the general tectonics and geology of this area are dealt with; the structures and the structural analysis of the area are studied.

1-1 *Tectonic setting of the study area*

Some of the Arabia-Eurasia convergences are accommodated in the Zagros Mountains of SW Iran, while most of the rest is taken up in the seismic belts of the Central Caspian, the Alborz and the Kopeh Dag of northern Iran, as Central Iran itself is relatively flat aseismic and probably rigid. Whatever shortening is not taken up in the Zagros must be expressed as N-S right lateral shear between central Iran and Afghanistan. This shear is manifest by major N-S right lateral fault systems on both the west (in Kerman Province) and east (in Sistan) sides of the Dasht-e-Lut, another flat aseismic rigid block (Fig1).

The overall Arabia-Eurasia convergence is known from a combination of Africa-Eurasia and Arabia-Eurasia motions to be approximately N-S in Eastern Iran, with rates of about 30 mm/ year at 50˚E and 40 mm/year at 60˚E (Jackson, 1992; DeMets et al., 1994; Jestin et al., 1994; Chu and Gordon, 1998). Central Iran is a mosaic of various tectonic blocks once separated by minor ocean basins (Berberian and King, 1981) that started to close in the mid-Tertiary (McCall, 1996). Much of the broader collision zone, however, did not start to deform until the Mid-Miocene or even later (Dewey et al., 1986).

***Correspondence Author:** Mehran Arian, Department of Geology, Science and Research Branch, Islamic Azad University, Tehran, Iran. Email: mehranarian@yahoo.com

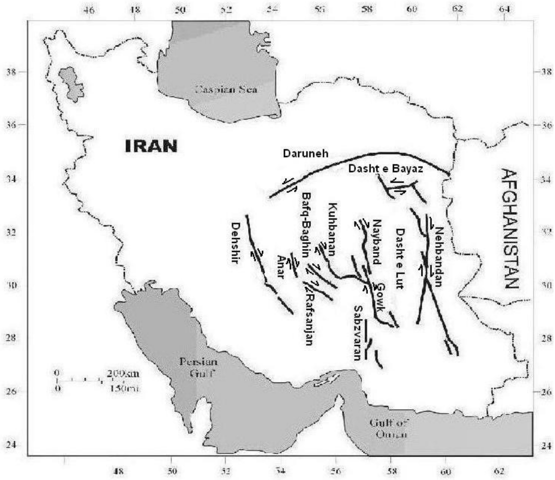

Fig1. Major faulting in Central Iran. The east and west faults of Dasht-e-lut are right lateral Strike slip.

In particular, major deformation of the Zagros folded belt appears that doesn't have begun until the Pliocene, approximate 5 Ma years ago or less (Falcon, 1974) , which is also the time at which there was a major re-organization of the sedimentation and deformation in the south Caspian Basin (Devlin et al., 1999; Jackson et al., 2002). We suspect this time represents the final closure of any remaining ocean basins and the onset of true intra-continental shortening within Iran. We also expect that the present-day configuration of active faulting dates from roughly this time. Jackson and McKenzie (1984, 1988) and Jackson et al. (1995) suggest that the Zagros accommodates about 10-15 mm/ year of present-day shortening. This estimation is very dependent on the assumptions they made, but is roughly compatible with approximate 50 km of shortening which have occurred in the folded belt of Zagros over the last 5 Ma (Falcon, 1969 & 1974).

Thus we expect that 20-25 mm/ year remains to be taken up north of the Zagros and to be represented as N-S shear in eastern Iran. This reasoning implies that a total of 100-125 km of right-lateral slip has occurred on the faults east and west of the Dasht-e-Lut over the last 5 Ma; the total offset may be more if the faults were active before 5 Ma (Jackson and Walker, 2001).

After the general retreat of the Seas in Iran at the late Jurassic which is related to tectonic events of late Cimmerian, the big advancement of sea in Barremian-Aptian occurred and the result is the sedimentation of Orbitoline limestone to lower Cretaceous which in the study area is situated on older formations as unconformity (Darakhshani, 1999).

Bafq-Baghin fault system has extended parallel to Bafq-Baghin Mountains that is located in the west of Dasht-e-Lut and in parallel with active and seismic fault of Kouhbanan in the northeast and Rafsanjan Fault in the southeast(Fig1). This fault is directed from northwest to southeast and is in the west of N-S active fault of Nayband-Gowk.

The available evidence is nonetheless sufficient to suggest that the probable slip rates (approximately 1-2 mm/ year) and total offset (approximate 12 km) on the Nayband-Gowk fault system are relatively small, and that most of the N-S shear between central Iran and Afghanistan is taken up on the eastern side of the Dasht-e-Lut (Jackson and Walker, 2001).

2-Remote sensing

Most of the regional structures are the faults that the effects of their multi-functional roles as controlling of factor structures and sediment conditions are obvious.

The tectonic interface and multi-behaviors of the crushed layers in reaction to events such as circular movements of the blocks, the repeated inversion of turning direction, vertical block movements or the inversion of normal faults' mechanism which might have been inverted or repelled in their later periods of activity are among the points which should be paid sufficient attention in order to have a complete analysis of the area.

For a better analysis of the region structures, TM Landsat Satellite digital Data has been used. By using Optimum Index Factor (OIF), the most suitable False Color Combination (FCC) (Sheffield, 1985; Chatterjee et al, 1996) was obtained.

To select the best possible three-band combination and Optimum Index Factor (OIF) for evaluated bands of TM, we use the following algorithm:

$$OIF= \frac{\sum_{k=1}^{3} sk}{\sum_{j=1}^{3} Abs(rj)}$$

sk: The resultant of the standard deviation for band K.
rj: The correlation co-efficient between two bands of the three-bands combination.

Three-band combination with greatest Optimum index factor has the most information (by applying variance in computation) and the least duplication rate (by applying correlation coefficient).

In the next stage, different detector filters of edge (Hi pass) and the effect of sun radiation were used. By using these filters, border between different units of Lithology become clearer and linear processes such as faults and important fractures of the region were identified. In the final stage, the picture of the region was put under a layer of vector and the identified structures were shown on the picture.

After processing satellite digital data, field studies were carried out to confirm the obtained results. A lot of the regional faults were identified for the first time in this research.

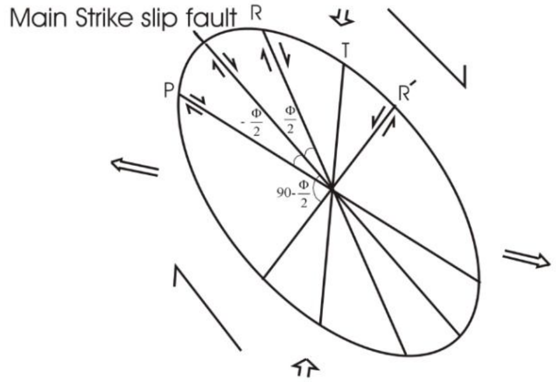

Fig2. Strain ellipsoid in convergent right lateral zone with five fractures.

3- Structural Analysis of the study area

Studies performed on the digital satellite data from the region and analyzing air photos and field work indicate that regional faults follow five main processes in right lateral shear zone, both in direction and in operation mechanism which may be formed in brittle shear zone (Fig5).

The first group of faults in the region is similar to "Y" faults in right lateral shear zone and has right lateral strike slip mechanism. They are formed in parallel direction with the main fault.

The second group have the same mechanism to the main fault but they make an angle of 15˚-20˚ ($\frac{\Phi}{2}$) (Φ: Angle of internal friction usually is considered 30˚) with the main fault in direction. The direction of these faults is in accordance with the direction of Riedel group in right lateral shear zone.

The third group of faults holds left shear components and has an angle of 60˚ to 80˚ ($90-\frac{\Phi}{2}$) with the main fault in direction and they are similar to anti-Riedel faults in the right lateral shear zone.

In the fourth group, the faults are at approximately –10˚ ($-\frac{\Phi}{2}$) angle with the main fault in direction and have a similar mechanism with the main fault. Their direction is in accordance with the faults in group P in the right lateral shear zone.

The fifth group of faults, directed at AZ 20º to 0º, show normal mechanism. They are similar to the faults in group T in the right lateral shear zone.

These shapes and structures form in brittle shear zones and the complete conformity of regional faults with these fractures proves right lateral simple shear with pressure component which affects the region (Fig2).

Shear fractures (R, R') form a complementary system in which R fractures are more extensive in comparison with R' fractures while R' shear with the advancement due to first basement fault operation have a fast rotation in comparison with R fractures and after some degrees of rotation may become locked and inactive.

R' fractures form only when R fractures cover each other (Naylor et al., 1986; Tchalenko & Ambraseys, 1970). P fractures are also formed by decrease in shear resistance of R fractures.

Since all basement movements are not absorbed by R fractures and between two shears of R, shortage axis inclines toward the fracture of R and also between the two covering R fractures, a small stress field which can be created new shear with an angle of $-\frac{\Phi}{2}$ in relation to the main movement (Naylor et al., 1986). Tension fractures are located in parallel with the shortage axis and they form the semi-angle between R and R'.

Another factor which can be taken into account to analyze regional structures is En echelon folds. Folds with strike slip faults are usually En echelon and oblique to the main side of shear. The term En echelon is related to structures' arrangement in a linear zone in such a way that folds or faults are parallel with each other with the same inclination towards the linear zone direction (Trace of fold axes in satellite image marked by —ı— for anticlines and —×— for synclines.)
Naming this type of folds is according to the folds which make movements at strike slip areas. In this region, we can find right handed folds because of the presence of the right lateral strike slip faults in the region (Sheikholeslami, 1994).

The direction of folds' axis can be useful for the recognition of the direction and displacement of right strike slip zone so that in the right lateral faults, folds incline towards right hand and in the left lateral faults; folds incline towards left hand (Fig 3). By using this method we can find strain geometry in simple shear form and anticipate the direction of R, R' shears, normal (T) and trust faults. In the early stages of deformation, simple En echelon folds are arranged and through the continuation of shear in the basement, they begin to rotate. In this state, the direction of these folds' axis which have an angle of 45˚as compared with the direction of shear in ideal conditions change to 10˚-35˚ in natural situations to the direction of the main fault. With the increase in displacement on strike slip zone, folds are separated from each other and some parts of folds also move around strike slip faults. With the continuation of block movements, semi-folds located around faults also move far away from the region (Harding & Lowell, 1979). These folds are clearly visible in the center of the highlands.

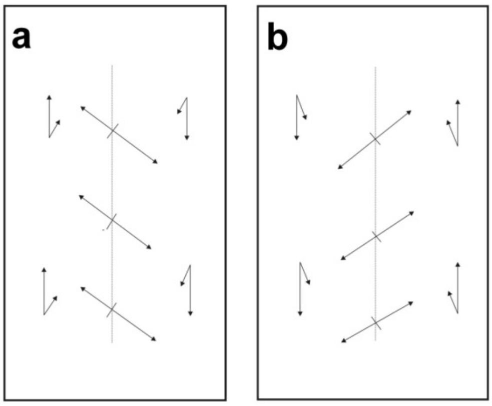

Fig3. (a) Schematic of right handed folds in the right lateral shear zone. (b) Schematic of left handed folds in the left lateral shear zone.

4- Segmentation of Bafq-Baghin fault system

60 fault segments on Bafq-Baghin fault system have been recognized by structural segmentation methods (Table1) (Fig4 to 8).
All of the fault segments in this system are right lateral strike slip with pressure component. Seven types of segment terminations have been determined that they have introduced below;
1- "Spurs between mountain and plain" The first type of fault segment termination has been recognized in the borders of:
F_8-F_9, F_9-F_{10}, F_{13}-F_{14}.
2- "En echelon with overlap or without overlap" The second type of fault segment termination has been recognized in the borders of:
F_1-F_2, F_{21}-F_{22}, F_{24}-F_{25}, F_{32}-F_{33}, F_{41}-F_{42}, F_{48}-F_{49}
3- "Cutted by minor fault" The third type of fault segment termination has been recognized in the borders of:
F_4-F_5 , F_6-F_7 ,F_7-F_8,F_{11}-F_{12},F_{14}-F_{15},F_{16}-F_{17}, F_{19}-F_{20} , F_{20}-F_{21} , F_{23} F_{24}-F_{27}-F_{28},F_{31}-F_{32},
‘ F_{57}-F_{58} , F_{58}-F_{59}. F_{33}-F_{34}, F_{34}-F_{35} , F_{35}-F_{36} , F_{36}-F_{37} , F_{37}-F_{38} , F_{38}-F_{39} , F_{39}-F_{40} , F_{40}-F_{41} , F_{42}-F_{43} , F_{49} -F_{50} , F_{51}-F_{52}, F_{52}-F_{53} , F_{53}-F_{54} , F_{54}-F_{55} , F_{55}-F_{56}‘F_{56}-F_{57}
4- "Fault Gaps" The forth type fault segment termination has been recognized in the borders of: F_2-F_3, F_{29}-F_{30}
5- "Sharp change in mountain front as bending" The fifth type fault segment termination has been recognized in the borders of :
F_3-F_4, F_5-F_6 ‘F_{15}-F_{16} ‘F_{22}-F_{23} ‘F_{25}-F_{26}, F_{30}-F_{31}, F_{43}-F_{44}, F_{44}-F_{45} ‘F_{45}-F_{46} ‘F_{59}-F_{60}
6- "Change of structures, plans and shapes of geology" The sixth type fault segment termination has been recognized in the borders of:
F_{17}-F_{18}, F_{18}-F_{19}, F_{46}-F_{47}, F_{47}-F_{48}
7- "Change of type and resistance of the rocks in borders between mountain and plain" The seventh type fault segment termination has been recognized in the borders of:
F_{10}-F_{11}, F_{12}-F_{13}, F_{26}-F_{27}

Table1. Characteristics of Bafq-Baghin fault system

Fault segment	Length (Km)	Atitude	Hanging wall lithology	Foot wall lithology
F_1	9.5	N40W	Cretaceous lime stone	Quaternary Alluvium
F_2	9	N18W70SW	Cretaceous lime stone	Quaternary Alluvium
F_3	2	N40W	Cretaceous lime stone	Quaternary old fans
F_4	2	N10W	Cretaceous lime stone	Quaternary old fans
F_5	1.5	N60W	Cretaceous lime stone	Quaternary old fans
F_6	7.5	N20W	Cretaceous lime stone	Quaternary old fans
F_7	3	N40W	Cretaceous lime stone	Quaternary old fans
F_8	4	N50W	Shemshak Formation(Triassic & Jurassic shale)	Quaternary old fans
F_9	5	N55W	Jurassic granite	Quaternary Alluvium and fans
F_{10}	18	N45W	Quaternary old Alluvium	Quaternary young Alluvium
F_{11}	3.5	N55W	Shemshak Formation(Triassic & Jurassic shale)	Quaternary old Alluvium
F_{12}	2	N45W	Shemshak Formation(Triassic & Jurassic shale)	Quaternary old Alluvium
F_{13}	2	N50W	Naiband Formation(Triassic lime stone)	Quaternary old fans
F_{14}	3.5	N35W	Naiband Formation(Triassic lime stone)	Quaternary old fans
F_{15}	3	N45W	Lalun Formation(Cambrian sand stone)	Naiband Formation(Triassic lime stone)
F_{16}	8	N30W	Quaternary fans	Quaternary fans
F_{17}	5.5	N40W	Quaternary and Tertiary fans	Quaternary and Tertiary fans
F_{18}	11.5	N60W	Tertiary marls	Tertiary marls
F_{19}	6	N50W80SW	Padeha Formation(Devonian lime stone)	Tertiary marls
F_{20}	20	N40W80SW	Lalun Formation(Cambrian sand stone)	Quaternary and Tertiary Alluvium
F_{21}	11.5	N35W85SW	Shotory Formation(Triassic dolomite)	Tertiary marls
F_{22}	4	N55W	Bahram Formation(Devonian lime stone)	Hojedk Formation(Jurassic shale)
F_{23}	3.5	N75W	Padeha Formation(Devonian lime stone)	Cretaceous lime stone
F_{24}	8	N40W	Bahram Formation(Devonian lime stone)	Hojedk Formation(Jurassic shale)
F_{25}	6	N55W	Hojedk Formation(Jurassic shale)	Hojedk Formation(Jurassic shale)
F_{26}	6	N60W	Hojedk Formation(Jurassic shale)	Mila Formation(Cambrian dolomite)
F_{27}	3.5	N40W	Hojedk Formation(Jurassic shale)	Ordovician dolomite
F_{28}	6	N35W	Ordovician dolomite	Bahram Formation(Devonian lime stone)
F_{29}	7.5	N20W	Cretaceous lime stone Lower	Cretaceous lime stone Middle
F_{30}	2.5	N5E	Quaternary Alluvium	Quaternary Alluvium
F_{31}	10	N12W	Cretaceous lime stone Middle	Quaternary old fans
F_{32}	2.5	N25W	Cretaceous lime stone Middle	Quaternary old fans
F_{33}	4	N30W	Cretaceous lime stone Middle	Quaternary young fans
F_{34}	4	N25W	Quaternary old Alluvium	Quaternary old Alluvium
F_{35}	4	N35W	Cretaceous lime stone Upper	Cretaceous lime stone Lower
F_{36}	5.5	N40W	Cretaceous lime stone Upper	Cretaceous lime stone Lower
F_{37}	2.5	N45W	Cretaceous lime stone Upper	Quaternary old fans
F_{38}	4	N40W	Quaternary Alluvium	Quaternary Alluvium
F_{39}	4.5	N55W	Quaternary fans	Quaternary fans
F_{40}	1.5	N25W	Cretaceous lime stone Lower	Cretaceous lime stone Lower
F_{41}	4.5	N50W	Cretaceous lime stone Lower	Cretaceous lime stone Lower
F_{42}	4	N35W	Cretaceous lime stone Lower	Quaternary old Alluvium
F_{43}	5.5	N40W	Cretaceous lime stone Lower	Quaternary old fans
F_{44}	5	N35W	Cretaceous lime stone Upper	Quaternary Alluvium
F_{45}	7	N45W	Quaternary young fans	Quaternary young fans
F_{46}	12	N60W	Quaternary young fans	Quaternary young fans
F_{47}	8.5	N25W75NE	Shemshak Formation(Triassic & Jurassic shale)	Shemshak Formation(Triassic & Jurassic shale)
F_{48}	3	N50W75NE	Dezu Formation(Cambrian shale)	Quaternary old fans
F_{49}	20	N45W75NE	Shemshak Formation(Triassic & Jurassic shale)	Quaternary fans
F_{50}	32	N50W	Hojedk Formation(Jurassic shale)	Quaternary fans
F_{51}	6	N50W	Ordovician Sand stone	Shemshak Formation(Triassic & Jurassic shale)
F_{52}	3.5	N25W	Niur Formation(Silurian dolomite)	Shemshak Formation(Triassic & Jurassic shale)
F_{53}	7	N45W	Niur Formation(Silurian dolomite)	Shemshak Formation(Triassic & Jurassic shale)
F_{54}	1	N87E	Niur Formation(Silurian dolomite)	Shemshak Formation(Triassic & Jurassic shale)
F_{55}	2.5	N45W80NE	Shotory Formation(Triassic dolomite)	Shemshak Formation(Triassic & Jurassic shale)
F_{56}	3	N50W80NE	Naiband Formation(Triassic lime stone)	Shemshak Formation(Triassic & Jurassic shale)
F_{57}	9.5	N60W	Shotory Formation(Triassic dolomite)	Shemshak Formation(Triassic & Jurassic shale)
F_{58}	1.5	N75W	Sardar Formation(Carbonifer lime stone)	Shemshak Formation(Triassic & Jurassic shale)
F_{59}	5.5	N55W	Shotory Formation(Triassic dolomite)	Shemshak Formation(Triassic & Jurassic shale)
F_{60}	3	N35W	Jamal Formation(Permian lime stone)	Shemshak Formation(Triassic & Jurassic shale)

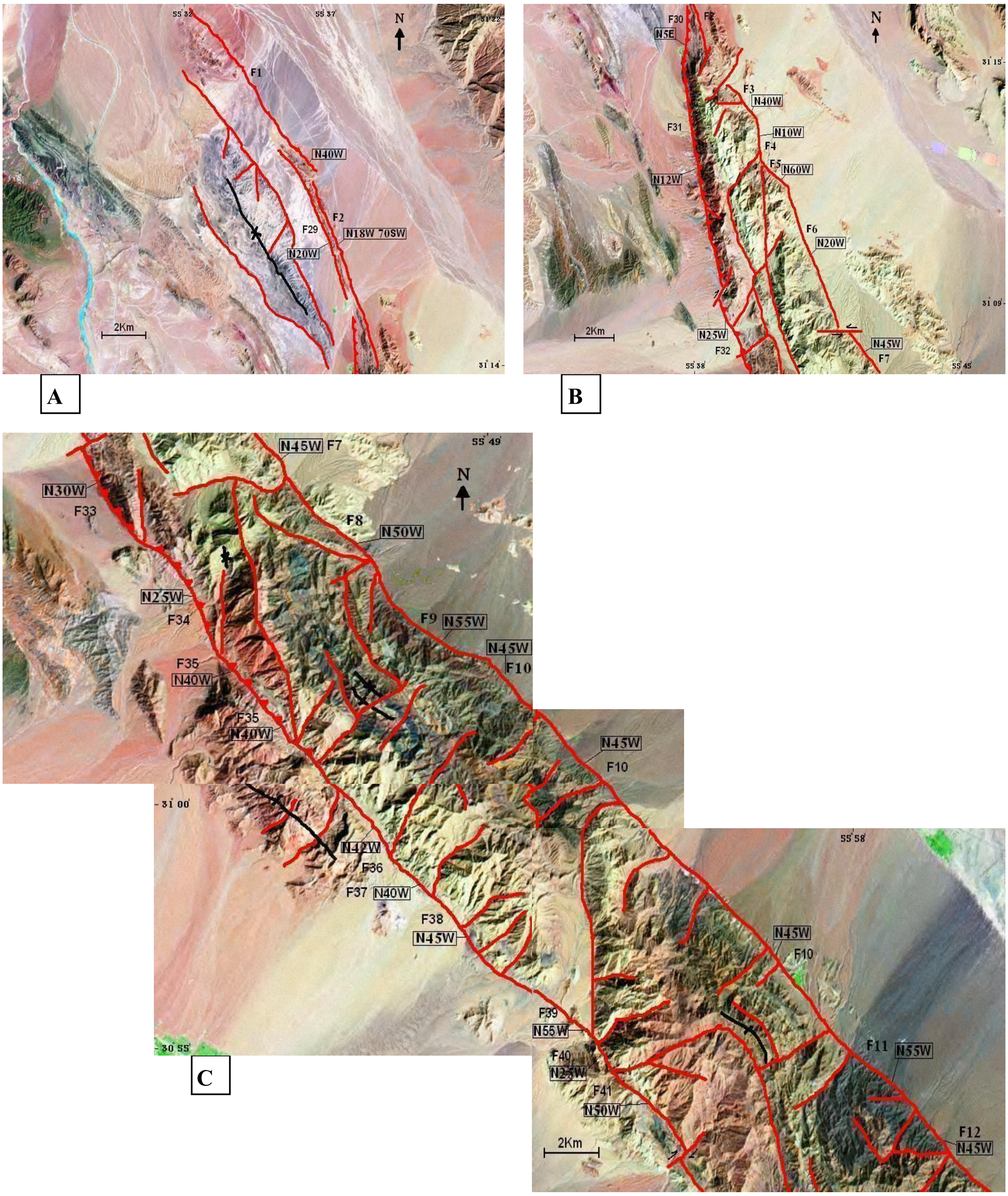

Fig4. Satellite image of NW part of Bafq-Baghin fault system
(A,B,C images are following and have same strike)

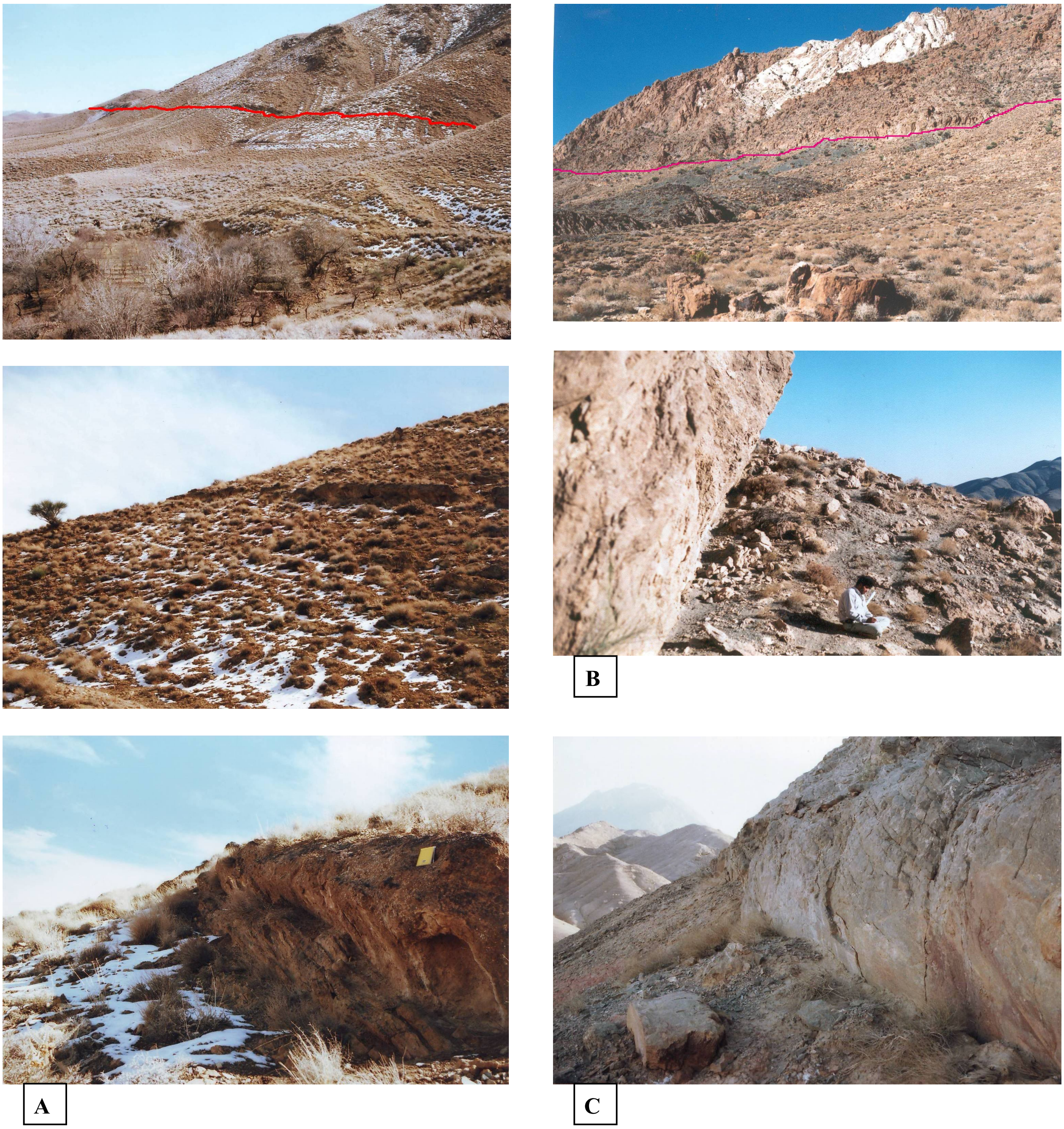

Fig5. Fault scarps of segments F19 (A), F56 (B), F2 (C).

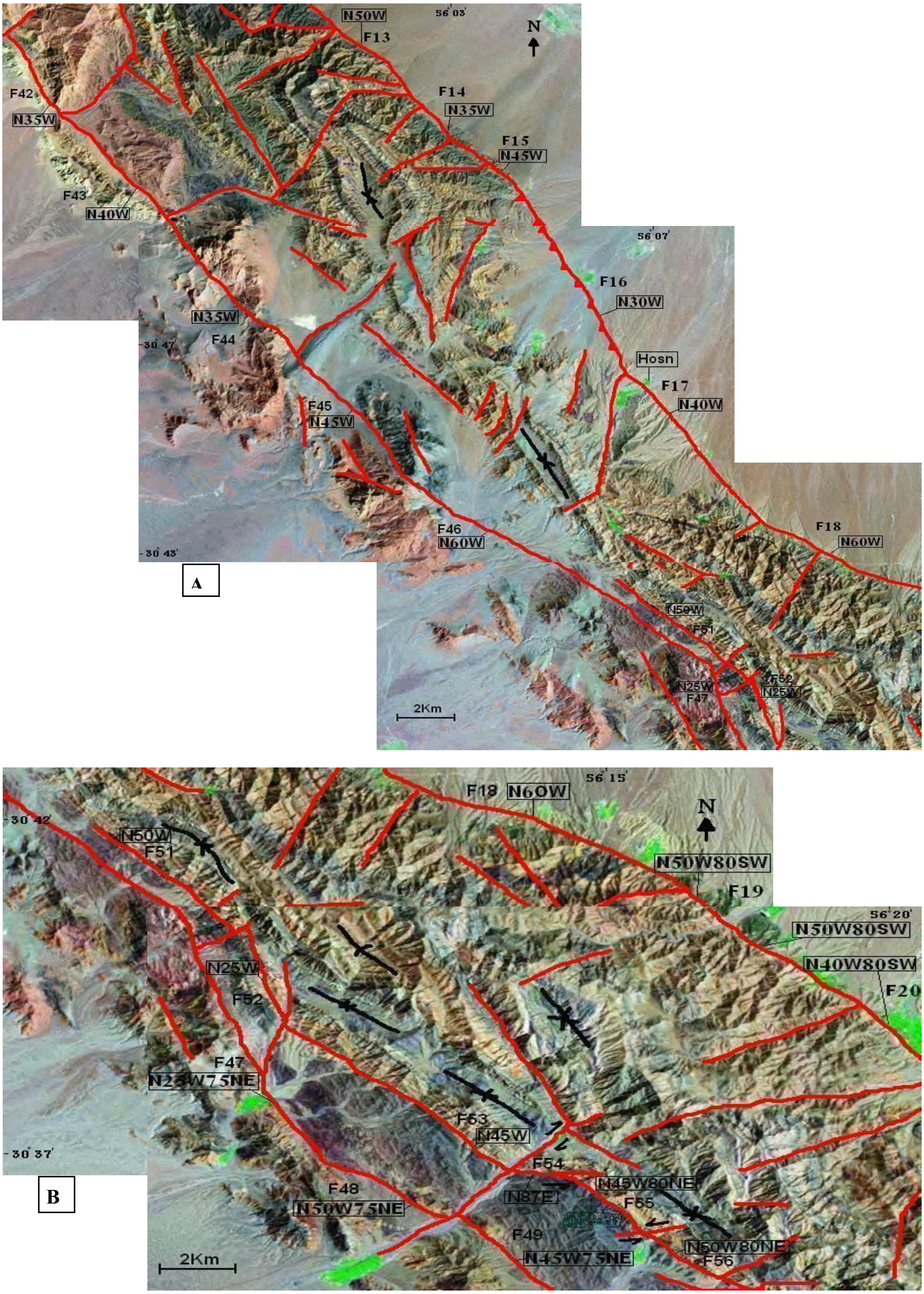

Fig6. Satellite image of center part of Bafq-Baghin fault system
(A, B images are following and have same strike)

A

B

Fig7. Fault segments of F20 (A), F19(B) Pass into alluvium fans

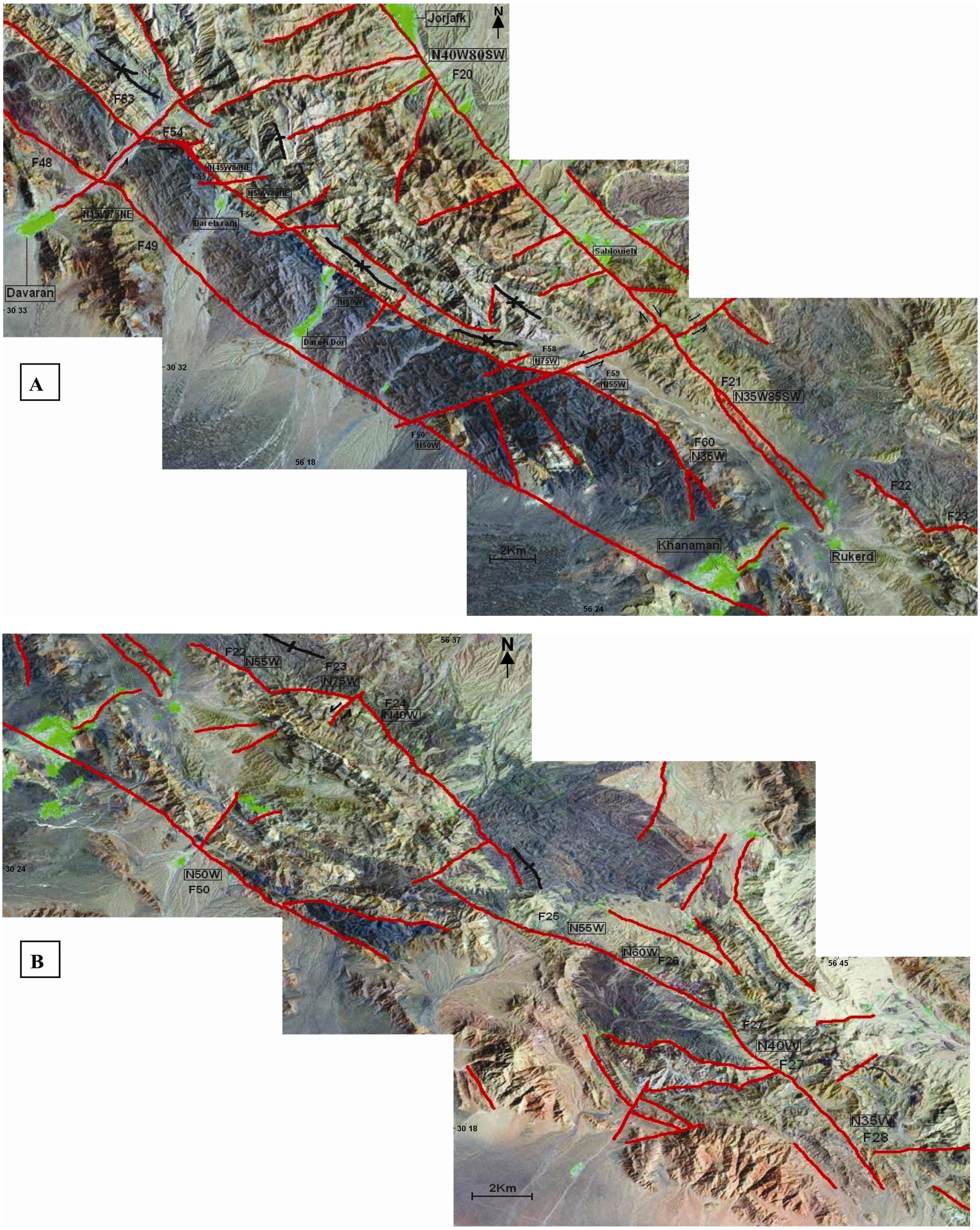

Fig8. Satellite image of SE part of Bafq-Baghin fault system
(A, B images are following and have same strike)

5- The seismicity of study area:

The study of the seismicity record in study area(Fig 9) shows that some of segments F_1,F_{13},F_{14},F_{18},F_{19},F_{20},F_{21},F_{49},F_{50},F_{58},F_{57},F_{59},F_{60} of the Bafgh-Baghin fault system have seismic records.
These earthquakes are generally located in almost the depth of 14 kilometer and their magnitude is from small to medium.

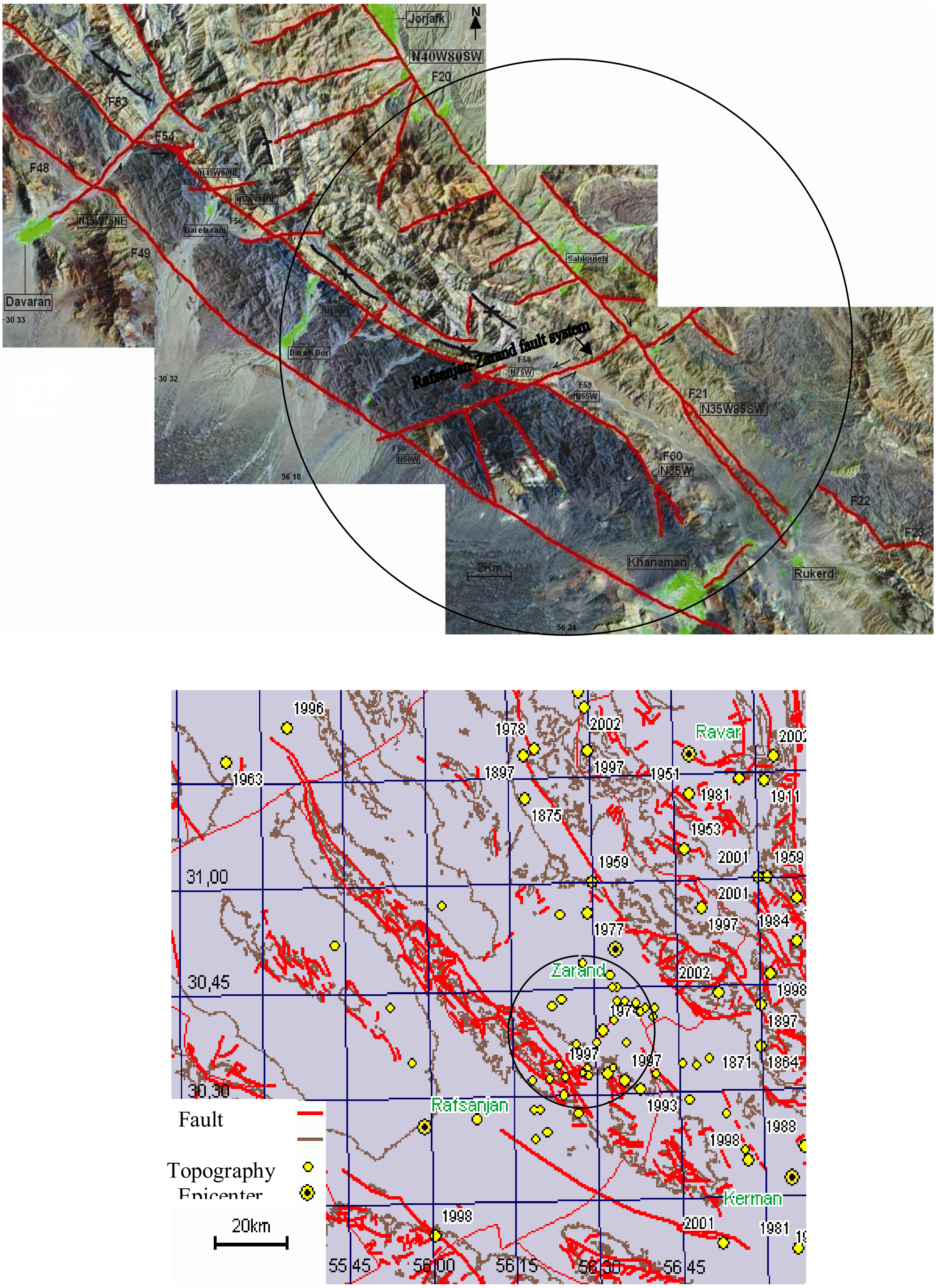

Fig9. Comparisons of the epicenter map of the recent earthquakes in the region with its landsat image.

Looking at the sedimentary cover in this region indicates that most of the earthquakes that happened have taken place are related to the upper of continental crust. Therefore, the occurrences of those big earthquakes have been known that there will be a longer returning period is not out of mind.

These earthquakes from the tectonic point of view are related to the expansion of a positive flower-like region in the interval of Bafgh-Baghin fault system and currently considering its trend in relation to the main local maximum principle stress (σ_1), it also includes right lateral shear. According the occurrence of multiple small earthquakes with a short returning period is referred to in the chart is expected.

Meanwhile the maximum seismic potential in the segments of fault system in Bafgh-Baghin has been calculated in the chart. The magnitude of the biggest moment of probable earthquakes (Mw) is based on Wells and Coppersmith equation (1994).

Mw=5/08+1/16 log (L)

Mw: the magnitude of the moment of the biggest probable earthquakes.

L: the length of the fault segment (kilometer)

Based on the calculations done in Table2, it will be seen that segments of F_{50}, F_{20}, F_{49}, F_{10}, F_{18}, F_{21} and F_{46} have the highest length and the seismic potential with magnitude of more than 6 too.

Meanwhile relative frequency of epicenter of earthquakes has taken place (cross form) in the southeast area of Bafgh-Baghin Mountain. It is related to the concentration of stress at the end of southeast magnetic lineaments F-559, F-557 and F-556(Fig10).

In fact, the seismic place in this study area is the intersection of the mentioned lineaments above. According to the studies of Talwani in 1999, shows that these areas are center of accumulations of strains. His study shows that the rate of the accumulation of strains in the intersection of fault regions in the intracontinental area is comparable with the borders of the plates.

On the other side, study of the landsat images show that there is a left lateral strike slip fault system with northeast – southwest trending in south eastern of study area. For the first time, it was introduced in this paper as Rafsanjan-Zarand lateral fault. The recent earthquakes in the region between Rafsanjan and Zarand are as a result of these fault activities.

Comparing the epicenter of the region earthquakes with the landsat images show that most of earthquake epicenters of the region (2005-2009) have northeast-southwest trend interrelated to the Rafsanjan-Zarand fault system (Fig9).

A part of this fault system has been intersected the strike of the Bafgh-Baghin Mountain as a cross form has a length of 12 kilometers. The function of this fault is left lateral strike slip that caused apparent movement in the rocky layers of the area. The concentration of epicenters of earthquake in this trend is mostly located at the intersection of this cross fault with the front fault which is on both sides and the center of the mountain and has turned the border between segments F_{20}-F_{21}, F_{49}-F_{50}, and F_{58}-F_{59} into fault. The existence of epicenters of earthquake in the strikes of Rafsanjan- Zarand fault system in alluviums indicates that the fault system is hidden in strikes of northeast and southeast. It is possible that in the future, there will be more powerful earthquakes, as a result of Rafsanjan-Zarand fault system function in the south and south-east of Zarand and parts of northeast of Rafsanjan.

Table2. Maximum seismic potential of Bafq-Baghin fault segments

No.	segment	(km) length	Mw	No.	segment	(km) length	Mw
1	F1	9.5	6.21	31	F31	10	6.24
2	F2	9	6.18	32	F32	2.5	5.54
3	F3	2	5.43	33	F33	4	5.78
4	F4	2	5.43	34	F34	4	5.78
5	F5	1.5	5.29	35	F35	4	5.78
6	F6	7.5	6.09	36	F36	5.5	5.94
7	F7	3	5.64	37	F37	2.5	5.54
8	F8	4	5.78	38	F38	4	5.78
9	F9	5	5.89	39	F39	4.5	5.83
10	F10	18	6.53	40	F40	1.5	5.29
11	F11	3.5	5.71	41	F41	4.5	5.83
12	F12	2	5.43	42	F42	4	5.78
13	F13	2	5.43	43	F43	5.5	5.94
14	F14	3.5	5.71	44	F44	5	5.89
15	F15	3	5.64	45	F45	7	6.05
16	F16	8	6.12	46	F46	12	6.33
17	F17	5.5	5.94	47	F47	8.5	6.16
18	F18	11.5	6.36	48	F48	3	5.64
19	F19	6	5.98	49	F49	20	6.59
20	F20	20	6.59	50	F50	13	6.37
21	F21	11.5	6.36	51	F51	6	5.98
22	F22	4	5.78	52	F52	3.5	5.71
23	F23	3.5	5.71	53	F53	7	6.05
24	F24	8	6.12	54	F54	1	5.08
25	F25	6	5.98	55	F55	2.5	5.54
26	F26	6	5.98	56	F56	3	5.64
27	F27	3.5	5.71	57	F57	9.5	6.21
28	F28	6	5.98	58	F58	1.5	5.29
29	F29	7.5	6.09	59	F59	5.5	5.94
30	F30	2.5	5.54	60	F60	3	5.64

The study of the aerial magnetic map in Rafsanjan indicates that the northeast flank of Bafgh-Baghin Mountain is controlled by the magnetic lineament of F-556 which conforms to the reaching the surface fault system in the Bafgh- Baghin area. However, three magnetic lineaments, F-559, F-557 and F-558, in the above mentioned southwest flank of the mountain is arranged from the northwest to the southeast. Meanwhile, under the mountain mentioned above, there is a long anti-cline basement called A-65 which based on the morphometrical indexes measurement, it is uplifting (Fig10).

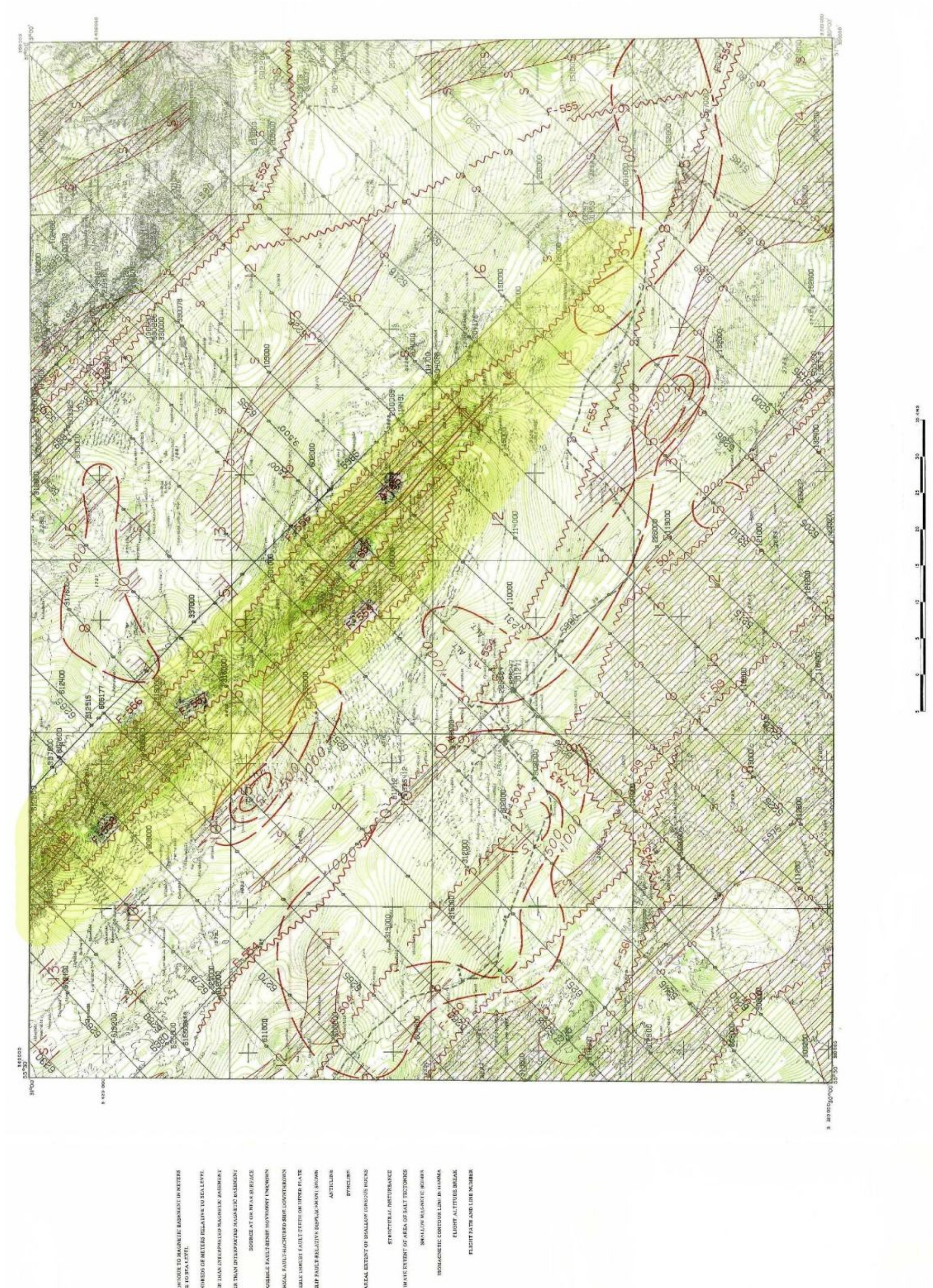

Fig10. Lineaments of the study region have been specified on the aerial magnetic map (GSI).

Conclusion

Bafq-Baghin Right lateral strike slip Fault which can be considered as an important fault in Central Iran with regard to its geometrical position in comparison with the other faults in the region has been considered the major fault of the region and it is the most important cause for the deformation of Rafsanjan northeast heights. High clarity of this fault sediment cut in the present period which is clearly shown in satellite digital data processing and field observation show the activeness of this fault. Other faults in this region have complete conformity with expected fractures in pressure shear zone.

These fractures include conjugated faults of Riedel and Anti-Riedel(R, R'), normal faults(T), faults parallel with the major fault(Y) and faults approximately parallel with the main fault(P).

Also the existence of right handed Enechelon folds prove a dominant transperssion in this region. Besides, the study of joints in a number of stations and with regard to the direction of faults in the study area and the direction of the folds' axis, we can obtain the direction of the maximum tension in the region in N20E- N25E direction which is a result of the convergence of Arabia towards Central Iran.

60 fault segments on Bafq-Baghin fault system have been recognized by structural segmentation methods. All of the fault segments in this system are right lateral strike slip with pressure component. Seven types of segment terminations have been determined. There are several recent epicenters that situated around of a new transverse lineament with NE-SW trending that introduced in this paper as left lateral strike slip Rafsanjan- Zarand fault system.

Acknowledgements

This work is funded by the Department of geology, Islamic Azad University, Science and Research branch, Tehran, Iran. Also, Special thanks to vice-president for research in Science and Research branch, Tehran.

REFERENCES

-Berberian, M., King, G.C.P., 1981. Towards a palaeogeograghy and tectonic evolution of

Iran. Canadian Journal of Earth Sciences 18, 210-265.

-Chatterjee, R. S., Roy, J. and Bhattacharya, A. K., 1996. Mapping geological features of the Jharia colfield from Landsat - 5 TM data, Int. J. Remote Sensing, vol. 17, No. 16, P. 3257-3270.

-Chu,D.,Gordon, R.G.,1998. Current plate motions across the Red Sea Geophysical Journal International 135,313-328.

-Darakhshani, R., 1999. Structural Analysis of Rafsanjan belt with emphasis morpho tectonical analysis of region, M.Sc. Thesis, University of Shiraz, 189

-Demets,C.,Gordon, R.G., Argus, D.F., Stein, S., 1994. Effect of recent revisions to the geomagnetic reversal time scale on estimates of current plate motions, Geophysical Research Letters 21, 2191-2194.

-Devlin, W.J., Cogswell, J.M., Gaskins, G.M., Isaksen, G.H., Pitcher, D.H., Puls, D.P., Stanley, K.O., Wall, G.R.T., 1999. south Caspian basin: young, cool, and full of promise. GSA Today 9, 1-9.

-Dewey, J.F., Hempton, M.R., Kidd, W.S.F., Saroglu, F., Sengor, A.M.C., 1986, Shortening of continental lithosphere; the neotectonics of eastern Anatolia, a young collision zone. Special Publication of the Geological Society London 19, 3-39.

-Falcon, N.L., 1969. Problems of the relationship between surface structure and deep displacements illustrated by the Zagros range, Special Publication of the Geological Society London 3, 9-22.

-Falcon, N.L., 1974. Southern Iran: Zagros Mountains. Special Publication of the Geological Society London 4, 199-211.

-GSI, Geology survey of Iran

-Harding,T.P. and Lowell,J.D. 1979. Structural styles, their plate tectonic habitats and hydrocarbon traps in petroleum province, Amer. Ass. Petr. Geol. Bull., Vol.63, 1016-1058.

-Jackson, J.A., 1992, Partitioning of strike-slip and convergent motion between Eurasia and Arabia in Eastern Turkey and the Caucasus. Journal of Geophysical Research 97, 12,471-12,479.

-Jackson, J., Haines, J., Holt, W., 1995. The accommodation of Arabia-Eurasia plate convergence in Iran. Journal of Geophysical Research 100, 15,205-15,219.

-Jackson, J., McKenzie, D., 1984. Active tectonics of the Alpine-Himalayan Belt between western Turkey and Pakistan. Geophysical Journal of the Royal Astronomical Society 77, 185-264.

-Jackson, J., McKenzie, D., 1988. The relationship between plate motions and seismic moment tensors, and the rates of active deformation in the Mediterranean and Middle East. Geophysical Journal 93, 45-73.

-Jackson, J., Walker, R., 2001, Offset and evolution of the Gowk fault, S.E. Iran: A major intra-continental strike-slip system, Journal of structural Geology 24 (2002) 1677-1698.

-McCall, G.J.H., 1996. The inner Mesozoic to Eocene ocean of south and Central Iran and associated microcontinents, Geotectonics 29, 490-499.

-Naylor, M.A., Mandl, G., and Sijpesteijn, C.H.K. 1986, Fault geometries in basement induced wrench faulting under different initial stress states. Jour. Sruct. Geol., Vol.8, PP. 737-752.

-Sheffield, C., 1985, Selecting band combinations from multispectral data, Photogrametric Engineering and Remote Sensing, Vol. 51, No.6.

-Sheikholeslami, M., 1994. Analysis of tectonic and seismotectonic in Davaran region (northeast of Rafsanjan). M.Sc. Thesis, Azad university of Tehran north, 147.

-Tchalenko, J.S., 1970, Similarities between shear zones of different magnitudes, Geol. Soc. Amer. Bull, Vol.81, PP.1625-1640.

-Tchalenko, J.S., and Ambraseys, N.N., 1970. Structural analysis of the Dasht-e-Bayaz (Iran) earthquake fractures. Geol. Soc. Amer. Bull., Vol.81, No.1, PP. 41-60.